Digital Control of Spinning Flexible Spacecraft

H. F. VanLandingham* and L. Meirovitch†
Virginia Polytechnic Institute and State University, Blacksburg, Va.

A procedure is presented for the active control of a spinning flexible spacecraft. Precision attitude control, as well as active damping of flexible modes, is accomplished with digital processing and quantized control. The nonlinear controller design is made feasible by a modal decoupling method in conjunction with spatial discretization. This permits the design of a state reconstructor that accepts measurements from rate gyros and accelerometers. Actuation of the controllers is based on the values of the reconstructed state variables. The complete design is illustrated for a specific spacecraft model.

I. Introduction

INCREASINGLY stringent requirements for precision attitude control and suppression of elastic-member vibration have led to an increasing sophistication in active control of flexible spacecraft.[1-5] The problem of simulating flexibility is critical to a practical design, since the number of degrees of freedom of the model can become intractably large. Recent developments in the modeling and analysis of gyroscopic systems are designed to render these tasks easier. In particular, Ref. 6 provides some guidelines as to how to effect a good simulation with only a limited number of degrees of freedom. In addition, Ref. 7 develops a decoupling procedure which makes feasible a relay-type controller design for a flexible gyroscopic system. This paper develops a general design procedure for direct digital relay control. In contrast to the method of Kuo et al.,[2] the present design is made directly from the initial model rather than a redesign of a preliminary continuous-data controller. This capability represents an additional advantage of the modal synthesis approach first presented in Ref. 5.

As shown in Ref. 5, the equations of motion can be written in the form

$$I\dot{x}(t)+Gx(t)=X(t)+U(t) \tag{1}$$

where x is the $2n$-dimensional state vector of generalized coordinates and velocities, I is a symmetric $2n\times 2n$ matrix, and G is a skew-symmetric $2n\times 2n$ matrix. The vector X includes external forces acting on the system, such as impulsive forces of random amplitudes, and the vector $U(t)$ represents the generated generalized control forces.

The design of a digital controller presupposes an onboard computer. In addition, the dynamics of Eq. (1) must be modeled as a discrete-time system. Acceleration and velocity measurements are collected by the computer through analog-to-digital (signal) converters (ADC). Reference 9 provides details on the actual spatial location of the actuators and sensors. The measurement samples provide, in general, the necessary inputs to the computer to reconstruct the dynamical behavior of the spacecraft model. The digital control signals are, in turn, generated and transmitted to the actuators through digital-to-analog converters (DAC). For simplicity, only one type of control law will be used in this paper. Relay-type control signals are used to apply a sequence of quantized actuator command signals. The complete system configuration is shown in the diagram of Fig. 1.

Previous work has been concentrated on various specific aspects of the overall design problem. A general modeling procedure was given in Ref. 5, along with application to both linear state-variable feedback control and a nonlinear quantized control law. In Ref. 9, a study was made on the physical distribution of sensors and actuators required to effect control over both spacecraft attitude and a preselected number of elastic member deformation modes.

In response to a growing interest in computer-based control algorithms, an effort is made in this paper to relate the control procedures of Ref. 5 specifically to digital control. The topics discussed in this paper are the discrete-time modeling of the spacecraft dynamics in decoupled form, the design of a discrete-time-observer and quantized control signals in Sec. II; the application of the digital observer-based control to a specific spacecraft structure using a quantized control law in Sec. III; and Sec. IV, a discussion of the results, including responses during controlled and uncontrolled periods.

II. Discrete-Time Observer-Based Control

From the diagram of Fig. 1 it is clear that physical measurements taken on the spacecraft must be used to provide information to the observer subsystem. For the present purposes these measurements are assumed to be taken periodically every τ seconds. Referring to Fig. 1, if the controller is to be implemented by an onboard computer, then the measurements taken at $t=t_0$ must be processed in time to issue a new control command to the thrusters at $t=t_0+\tau$. Thus, all of the calculations of one control cycle must take less than τ seconds. This may be possible for low-order system but not for higher-order models. However, we cannot expect a reasonably accurate model of a flexible spacecraft to be of low order. Hence, a decoupling approach must be used. The approach used here is based on the development of Ref. 7. Introducing the linear transformation

$$x=Pw \tag{2}$$

into Eq. (1), where P is the normalized modal matrix satisfying $P^TIP=1$, the following decoupled form for the plant (spacecraft) dynamics is obtained:

$$\dot{w}=A_0w+B_0U \tag{3}$$

$$y=C_0\dot{w} \tag{4}$$

where $B_0=P^T$ and $A_0=P^TG^TP$ is a block-diagonal matrix.[5] Note that Eq. (4) is the assumed form of the measurements.

Presented as Paper 77-1099 at the AIAA 1977 Guidance and Control Conference, Hollywood, Fla., Aug. 8-10, 1977; submitted Sept. 21, 1977; revision received Jan. 27, 1978.

Index category: Spacecraft Dynamics and Control.

*Associate Professor, Department of Electrical Engineering. Member AIAA.

†Professor, Department of Engineering Science and Mechanics. Associate Fellow AIAA.

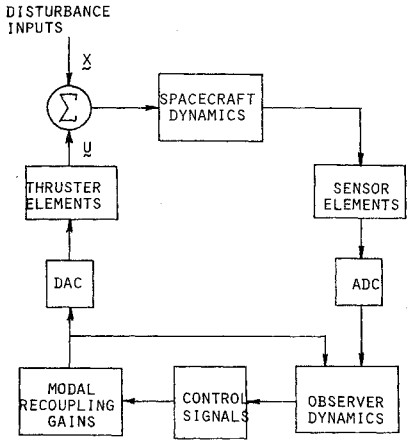

Fig. 1 Digital control system configuration.

Since the control inputs are held constant over τ intervals, a discrete-time model equivalent to the continuous-time system of Eqs. (3) and (4) can be used, namely

$$w(k+1) = \Phi_0 w(k) + \Gamma_0 U(k) \tag{5}$$

$$y(k) = Cw(k) + DU(k) \tag{6}$$

where

$$\Phi_0(\tau) = \exp\{A_0 \cdot \tau\} \tag{7}$$

is still block-diagonal and

$$\Gamma_0(\tau) = \int_0^\tau \Phi_0(t) B_0 \mathrm{d}t \tag{8}$$

and

$$C = C_0 A_0 \qquad D = C_0 B_0 \tag{9}$$

Equations (5-9) comprise the discrete-time model for the spacecraft dynamics. If this model provides reliable results between control inputs $U(k)$ and measured outputs $y(k)$ for $k=0,1,2,\ldots$, i.e., if it duplicates actual system performance under identical conditions, then a deterministic observer algorithm can be programmed into the computer to regenerate the state vector $w(t)$ at the sample instants $t=k\tau$ for $k=0,1,2,\ldots$.

Deterministic Observer

An observer system is a conceptual system which receives both the plant input and output measurements for the purpose of generating a vector $\hat{w}(t)$ that approaches $w(t)$ asymptotically.

Let us assume a discrete-time observer model of the general linear form

$$\hat{w}(k+1) = M\hat{w}(k) + LU(k) + Ky(k) \tag{10}$$

where the matrices M, L, and K are to be specified subsequently. Defining the error vector

$$\epsilon(k+1) = w(k+1) - \hat{w}(k+1) \tag{11}$$

and inserting Eqs. (5, 6, and 10) into Eq. (11), we obtain

$$\epsilon(k+1) = \Phi_0 w(k) + \Gamma_0 U(k) - M\hat{w}(k) - LU(k) - KCw(k) - KDU(k) \tag{12}$$

which simplifies to

$$\epsilon(k+1) = (\Phi_0 - KC) w(k) + (\Gamma_0 - L - KD) U(k) - M\hat{w}(k) \tag{13}$$

At this point, we set

$$L = \Gamma_0 - KD \qquad M = \Phi_0 - KC \tag{14}$$

whence we obtain the error dynamics

$$\epsilon(k+1) = (\Phi_0 - KC)\epsilon(k) \tag{15}$$

The observer, Eq. (10), will be complete as soon as the matrix K is specified. Equation (15) provides us with the proper direction for specifying the matrix K. When the system of (5) and (6) satisfies the necessary and sufficient condition for observability, namely, when

$$\operatorname{rank}\begin{bmatrix} C \\ C\Phi_0 \\ \hline C\Phi_0^{N-1} \end{bmatrix} = N \tag{16}$$

when N is the order of the system (see Ref. 8), then the parameters (entries) of K control every eigenvalue of $(\Phi_0 - KC)$. Thus, for a fast responding observer, K can be specified so that the magnitudes of the eigenvalues of $(\Phi_0 - K)$ are much smaller than one.

Stochastic Observer

In any given situation, however, the dynamics of the spacecraft will not be known exactly. To allow for modeling and measurement errors, we incorporate the discrete-random processes $n(k)$ and $w(k)$ as additive terms in Eqs. (5) and (6), respectively. Assuming for convenience that these plant and measurement error sources are stationary, zero-mean Gaussian processes with covariance matrices Q and R, respectively, the gain matrix $K(k)$ can be calculated to minimize the mean-squared error $\epsilon(k)$. This optimal gain $K(k)$ is given by[10]

$$K(k) = \Phi_0 V(k) C^T [CV(k)C^T + R]^{-1} \tag{17}$$

where $V(k)$ is the matrix of $w(k)$, satisfying

$$V(k+1) = [\Phi_0 - K(k)C] V(k) \Phi_0^T + Q \tag{18}$$

The gain $K(0)$ in Eq. (17) requires the initial condition $V(0)$ for Eq. (18), where $V(0)$ is the covariance matrix for the initial vector $w(0)$. Equations (17) and (18) represent calculations which may be done prior to "running" the observer. Very often, to simplify the computations, the steady-state gains are used, i.e., the K matrix which corresponds to the steady-state solution of Eq. (18).

To complete the closed-loop control of Fig. 1, the computer must generate the proper control signals which, in turn, become the actuator commands. The manner in which complete controllability of the system is ascertained is similar to the condition, Eq. (16), for complete observability. A necessary and sufficient condition for the system of Eqs. (5) and (6) to be completely controllable is that[8]

$$\operatorname{rank}[\Gamma_0 \ \Phi_0\Gamma_0 \ \Phi_0^2\Gamma_0 \ldots \Phi_0^{N-1}\Gamma_0] = N \tag{19}$$

Exact relationships are developed in Ref. 9 between point forces and torques acting on a specific spacecraft structure and the corresponding generalized forces [$U(t)$ of Eq. (1)] for that model. For present purposes, the details of modeling associated with measurement and actuation, i.e., the derivation of matrices B_0 and C_0 of Eqs. (3) and (4), are bypassed in favor of illustrating the computation involved in digital control.

Controller Design

The quantized control presented in this paper represents a modified relay-type control. It is noted that a given mode of

the decoupled system, Eq. (3), represents a second-order linear oscillator. On each of the decoupled modes, we specify a nonlinear control which is dependent on one of the generalized coordinates. The principal advantage of quantized control over linear control is its ability to perform the control action without operating continuously. The actuators are required to operate only in short bursts, making it a practical control law in terms of control jets currently used in spacecraft attitude control.

The specific quantized control law presented here is adapted from the on-off control of Ref. 5. For each mode a region of deadband is assumed, based on the recognition that within some tolerance small oscillations are acceptable. By sensing the velocity component of each oscillation mode from the observer output, a relay control law can be established as a preliminary actuation signal for that mode. Hence, for the rth mode the control function is

$$u_r = \begin{cases} -k_r & \eta_r > d_r \\ 0 & |\eta_r| \le d_r \\ k_r & \eta_r < -d_r \end{cases} \tag{20}$$

which is used conceptually to drive the rth decoupled mode to a minimal value specified by the deadband parameter d_r. The rate at which the rth mode variation is regulated depends on the thrust-level parameter k_r. Figure 2 illustrates the effect of u_r in Eq. (20) applied to the dynamics of the decoupled rth mode, i.e., the natural response of the nonlinear equations

$$\dot{\xi}_r(t) - \omega_r \eta(t) = 0$$
$$\dot{\eta}_r(t) + \omega_r \xi_r(t) = u_r/\omega_r \tag{21}$$

Note that the designer has the means to affect both the rate of amplitude decay and the ultimate maximum amplitude of mode oscillation. No provision has been made for any internal damping due to the material deformation, under the assumption that this effect is small. The explicit solution of Eq. (21), corresponding to the phase-plane trajectory of Fig. 2, can be found in Ref. 5.

Referring again to Fig. 1, it is noted that the on-off control signals were developed for the uncoupled modes and not for the original state vector x. We complete the closed-loop control system by combining the on-off control signals to obtain the actuator commands for the spacecraft. The nature of the actuator control signals is quantized both in time and in amplitude. As a practical point, the amplitude quantization can be made coarser in order to reduce the required number of actuator levels.

Assuming that Eq. (19) is satisfied, the actuation signals will be sufficient to control the modes of the truncated model. In the next section a relatively simple, yet nontrivial, spacecraft structure is considered. Using this specific spacecraft example, we will focus on the details necessary for a digital controller design. Following the example design section, a comparison of simulated results is made illustrating the effects of control in reducing the amplitudes of the elastic modes of vibration.

III. Example of Spacecraft Control

In this section we consider the control of the spacecraft in Fig. 3. We shall assume that the center of mass of the structure coincides with the center of mass P of the platform, that there are no members rotating relative to the platform, and that the two elastic panels attached to the platform are symmetric with respect to the point P. Following the derivation in Ref. 5, Lagrange's equations of motion yield an analytical model of the form

$$m\ddot{q}(t) + g\dot{q}(t) + kq(k) = Q(t) \tag{22}$$

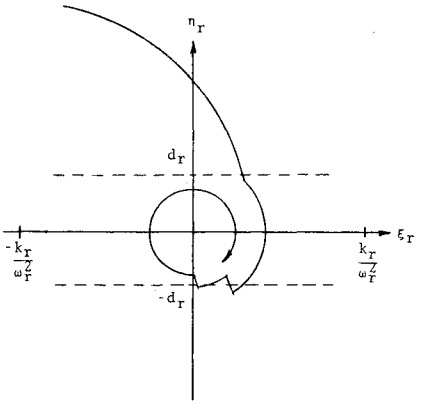

Fig. 2 Phase plane trajectory for the rth mode.

where the configuration vector

$$q(t) = [\theta_1(t)\ \ \theta_2(t)\ \ \zeta_1(t)\ \ \zeta_2(t)\ \ \zeta_3(t)]^T \tag{23}$$

consists of the nutation angles θ_1 and θ_2, the first about x_p and the second about y_p; ζ_1, the first out-of-plane mode amplitude of the elastic panel; ζ_2, the first in-plane bending mode amplitude; and ζ_3, the first torsional mode about x_p. Here we have used the notation x_p and y_p to represent the platform axes with origin at P in Fig. 3. For this example, we assume that in equilibrium the platform axes $x_p y_p z_p$ rotate relative to the inertial space XYZ with the uniform angular velocity Ω about z_p, where z_p is parallel to Z. The coefficient matrices m, g, and k are given by

$$m = \begin{bmatrix} A & 0 & 0 & 0 & e \\ 0 & B & -b & 0 & 0 \\ 0 & -b & m_1 & 0 & 0 \\ 0 & 0 & 0 & m_2 - \dfrac{a^2}{C} & 0 \\ e & 0 & 0 & 0 & m_3 \end{bmatrix} \tag{24}$$

$$g = \Omega \begin{bmatrix} 0 & C-A-B & 0 & 0 & 0 \\ A+B-C & 0 & 0 & 0 & 0 \\ 0 & 0 & 0 & 0 & 0 \\ 0 & 0 & 0 & 0 & 0 \\ 0 & 0 & 0 & 0 & 0 \end{bmatrix} \tag{25}$$

$$k = \Omega^2 \begin{bmatrix} C-B & 0 & 0 & 0 & e \\ 0 & C-A & -b & 0 & 0 \\ 0 & -b & m_1\lambda_1^2 & 0 & 0 \\ 0 & 0 & 0 & m_2(\lambda_2^2 - 1) & 0 \\ e & 0 & 0 & 0 & m_3\lambda_3^2 \end{bmatrix} \tag{26}$$

where λ_i is Λ_i/Ω, $i = 1,2,3$. The specific parameter values were taken or calculated to be

$A = 1500$ kg cm^2, $B = 7000$ kg cm^2
$C = 10{,}000$ kg cm^2, $\Omega = 0.6$ rad s^{-1}
$m_1 = 0.436$ kg, $m_2 = 0.175$ kg, $m_3 = 0.064$ kg
$e = 5.23$ kg, $b = 51.2$ kg, $a^2 = 57.63$ kg^2 cm^2

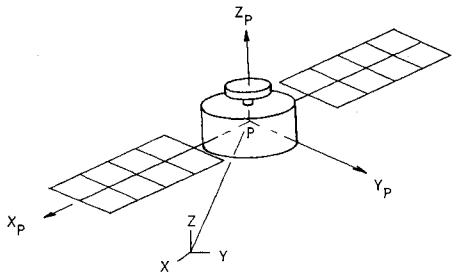

Fig. 3 Flexible spacecraft structure.

$\Lambda_1^2 = 4.59\ \text{rad}^2\ \text{s}^{-2}$, $\Lambda_2^2 = 11.44\ \text{rad}^2\ \text{s}^{-2}$
$\Lambda_3^2 = 31.5\ \text{rad}^2\text{s}^{-2}$

See Ref. 5 for the physical definitions of the parameters.

The second-order vector equation (22) is easily converted into the form of Eq. (1) by defining the state vector

$$x(t) = [\dot{q}^T(t) \quad q^T(t)]^T \tag{27}$$

whence,

$$I = \left[\begin{array}{c|c} m & 0 \\ \hline 0 & k \end{array}\right] \qquad G = \left[\begin{array}{c|c} g & k \\ \hline -k & 0 \end{array}\right] \tag{28}$$

Solving the eigenvalue problem, we find the five spacecraft frequencies:

$\omega_1 = 0.600\ \text{rad s}^{-1}$ $\omega_2 = 0.925\ \text{rad s}^{-1}$
$\omega_3 = 3.356\ \text{rad s}^{-1}$ $\omega_4 = 5.565\ \text{rad s}^{-1}$
$\omega_5 = 6.697\ \text{rad s}^{-1}$

If we now follow the development of Sec. II, we recognize the coefficient matrix A_0 in Eq. (3) as

$$A_0 = \text{block-diag}\left[\begin{array}{cc} 0 & \omega_i \\ -\omega_i & 0 \end{array}\right] \tag{29}$$

for $i = 1,2,\ldots5$. And after calculating the modal matrix P,

$$B = P^T = \left[\begin{array}{cccccccccc} 0.010 & 0 & 0 & 0 & 0 & 0 & 0.017 & 0 & 0 & 0 \\ 0 & 0.010 & 0 & 0 & 0 & -0.017 & 0 & 0 & 0 & 0 \\ 0 & 0.006 & -0.092 & 0 & 0 & 0.025 & 0 & 0 & 0 & 0.034 \\ 0.023 & 0 & 0 & 0 & 0.031 & 0 & -0.006 & 0.099 & 0 & 0 \\ 0 & 0 & 0 & 0 & 0 & 0 & 0 & 0 & 0.719 & 0 \\ 0 & 0 & 0 & 2.41 & 0 & 0 & 0 & 0 & 0 & 0 \\ 0 & 0 & 0 & 0 & -0.856 & 0 & 0.005 & 0.709 & 0 & 0 \\ 0 & 0.029 & 3.95 & 0 & 0 & 0 & 0 & 0 & 0 & 0.154 \\ 0 & -0.007 & -0.875 & 0 & 0 & -0.003 & 0 & 0 & 0 & 0.690 \\ -0.017 & 0 & 0 & 0 & 4.62 & 0 & 0.001 & 0.131 & 0 & 0 \end{array}\right] \tag{30}$$

which represents the input matrix for each of the generalized forces acting on the system. If we further assume that

$$C_0 = [I \mid 0]P \tag{31}$$

which corresponds to a separate measurement for each modeled vibrational mode, then the decoupled continuous-time system of Eqs. (3) and (4) is complete.

It is clear that by introducing Eq. (29) into Eq. (7) we obtain the expression

$$\Phi_0(\tau) = \text{block-diag}[\phi(\omega_i\tau)] \tag{32}$$

where

$$\phi(\omega_i\tau) = \left[\begin{array}{cc} \cos\omega_i\tau & \sin\omega_i\tau \\ -\sin\omega_i\tau & \cos\omega_i\tau \end{array}\right]$$

for $i = 1,2,\ldots,5$.

The sample interval is taken to be $\tau = 0.01$ s. This together with the natural frequencies ω_i, $i = 1,2,\ldots,5$ just listed, specifies Φ_0. Calculations based on Eqs. (8) and (9) for Γ_0, C, and D yield the remaining discrete-time model coefficient matrices.

At this point, the observability and controllability criteria of Eqs. (16) and (19) could be checked. We dispense with this formality here only because the assumed physical measurements and generalized input forces insure both of these system properties. Thus, for this example, we know in advance that the system is amenable to feedback control.

For simplicity, we use the deterministic observer formulation of Eqs. (10) and (14) with a constant gain matrix K specified so that the observer eigenvalues are:

$$\{0.995, 0.995, 0.992, 0.992, 0.990, 0.990, 0.988, 0.988, 0.961, 0.961\} \tag{33}$$

A relatively slow responding observer was used to illustrate the distinction between the actual mode variations and their reconstructed values.

For the control and simulation phase, the initial values were taken to be:

$\theta_1(0) = \theta_2(0) = 0$
$\dot{\theta}_1(0) = \dot{\theta}_2(0) = 10^{-4}\ \text{rad s}^{-1}$
$\zeta_i(0) = 0,\ i$
$\zeta_2(0) = 0,\ \zeta_1(0) = \zeta_3(0) = 0.02\ \text{cm s}^{-1}$

and the control parameters were chosen to be

$$d_1 = d_2 = d_3 = d_4 = d_5 = 10^{-3}$$

$$k_i/\omega_i^2 = 0.0015\ \text{s}^{-2},\ i = 1,2,3,4$$

$$k_5/\omega_5^2 = 5 \times 10^{-4}\ \text{s}^{-2}$$

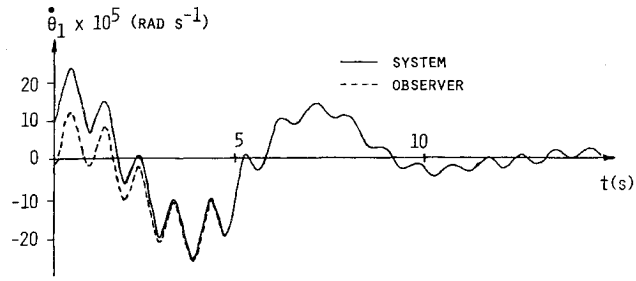

Fig. 4 Variation of the platform angular velocity $\dot{\theta}_1$ and its observed value $\hat{\dot{\theta}}_1$.

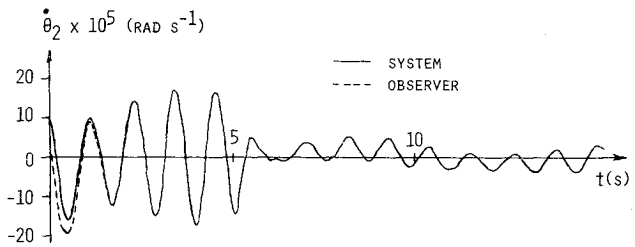

Fig. 5 Variation of platform angular velocity $\dot{\theta}_2$ and its observed value $\hat{\dot{\theta}}_2$.

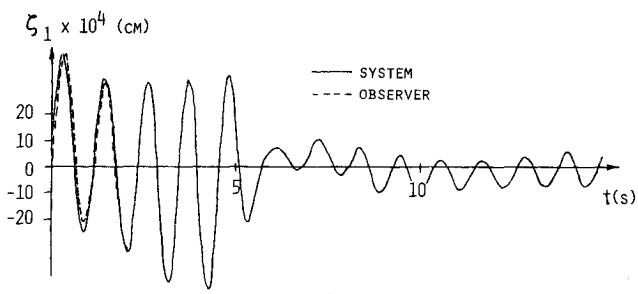

Fig. 6 Variation of first out-of-plane bending mode amplitude ζ_1 and its observed value $\hat{\zeta}_1$.

IV. Results and Conclusions

With the model and parameter values as outlined in the previous section, simulations were made of the system response. In particular, comparisons are given between controlled and uncontrolled behavior.

Discussion of Results

In Figs. 4 and 5 the variations in the platform angles of rotation are shown. The simulation was made to illustrate two phenomena. The first is the difference between the actual angle and the corresponding reconstructed angle (shown as a dashed line); the second is the effect of applying the controls to the system. For the first 5 s the response is uncontrolled. At time $t=5$ s the controls are applied, thereby decreasing the vibration amplitude. The deadband associated with the nonlinear control allows certain low levels of mode amplitudes to be undamped by the active control. Since there will always be some acceptable nonzero tolerance on the vibrations, no attempt was made to drive the oscillations to zero. The quantized control parameters were set only to effect a significant amplitude decrease, thereby illustrating the efficacy of the controller.

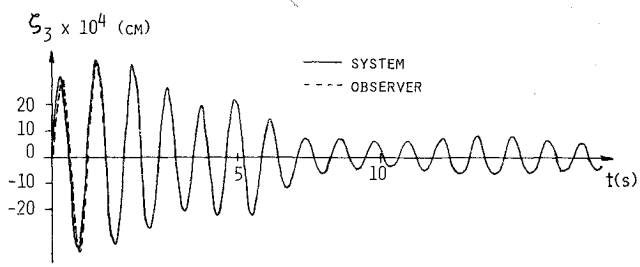

Fig. 7 Variation of first torsional mode amplitude ζ_3 and its observed value $\hat{\zeta}_3$.

The responses shown in Figs. 6 and 7 are the first out-of-plane bending mode amplitude ζ_1 and the first twist mode amplitude ζ_3, respectively. These plots are similar to Figs. 4 and 5 in that the response is uncontrolled for the first 5 s.

Conclusion

The modal synthesis control method of Ref. 5 has been extended to direct digital control. The computational advantages of controlling on the decoupled system observer have been illustrated by the quantized control law, which was derived from relay control of the decoupled second-order system blocks. An additional benefit of quantized control is its capability of being implemented by physical thruster elements.

Acknowledgment

The authors would like to acknowledge the help of Hayrani Öz of the Department of Engineering Science and Mechanics, Virginia Polytechnic Institute and State University, for his help in obtaining the numerical results.

References

[1] Gevarter, W.B., "Basic Relations for Control of Flexible Vehicles," *AIAA Journal,* Vol. 8, April 1970, pp. 666-672.

[2] Kuo, B.C., Seltzer, S.M., Singh, G. and Yackel, R.A., "Design of a Digital Controller for Spinning Flexible Spacecraft," *Journal of Spacecraft and Rockets,* Vol. 11, Aug. 1974, pp. 584-588.

[3] Poelaert, D.H.L., "A Guideline for the Analysis of a Nonrigid-Spacecraft Control System," *ESA/ASE Scientific and Technical Review,* Vol. 1, Jan. 1975, pp. 203-218.

[4] Porcelli, G., "Attitude Control of Flexible Space Vehicles," *AIAA Journal,* Vol. 10, June 1972, pp. 807-812.

[5] Meirovitch, L., VanLandingham, H.F. and Öz, H., "Control of Spinning Flexible Spacecraft by Modal Synthesis," *Proceedings of the International Astronautical Federation's 27th Congress,* Anaheim, Calif., Oct. 1976; also *Acta Astronautica,* Vol. 4, No. 9-10, 1977.

[6] Meirovitch, L. and Hale, A.L., "A Rayleigh-Ritz Approach to the Synthesis of Large Structures with Rotating Flexible Components," 13th Annual Meeting of the Society of Engineering Science, Inc., Hampton, Va., Nov. 1976; to appear in *Journal de Mècanique Appliquée.*

[7] Meirovitch, L., "A Modal Analysis for the Response of Linear Gyroscopic Systems," *Journal of Applied Mechanics,* Vol. 42, June 1976, pp. 446-450.

[8] Brogan, W.L., *Modern Control Theory,* Quantum Press, N.Y., 1974, Chap. 12.

[9] Meirovitch, L., VanLandingham, H.F. and Öz, H., "Distributed Control of Spinning Flexible Spacecraft," *Proceedings of the Symposium on Dynamics and Control of Large Flexible Spacecraft,* Blacksburg, Va., June 1977, pp. 249-269.

[10] Meditch, J.S., *Stochastic Optimal Linear Estimation and Control,* McGraw-Hill Book Co., N.Y. 1969, Chap. 5.